

Plasmonic Scattering Back Reflector for Light Trapping in Flat Nano-Crystalline Silicon Solar Cells

Supporting Information

Lourens van Dijk ^{*1}, Jorik van de Groep², Leon W. Veldhuizen³,
Marcel Di Vece¹, Albert Polman², Ruud E.I. Schropp³

E-mail: l.vandijk@uu.nl

¹Utrecht University, Nanophotonics - Physics of Devices, Debye Institute for Nanomaterials Science, High Tech Campus, Building 21, 5656 AE Eindhoven, The Netherlands

²FOM Institute AMOLF, Center for Nanophotonics, Science Park Amsterdam 104, 1098 XG Amsterdam, The Netherlands

³Eindhoven University of Technology (TU/e), Department of Applied Physics, Plasma and Materials Processing, 5600 MB Eindhoven, The Netherlands

Contents

1 Cell Fabrication	S2
2 Internal Quantum Efficiency	S3
3 Optical Modeling: Particle Swarm Optimization Algorithm	S4
References	S5

Figures: S1-S2

1 Cell Fabrication

The nc-Si solar cells are grown on flat Corning glass. The structure of the superstrate solar cell is: ZnO:Al/*p*-type nc-Si:H/intrinsic nc-Si:H/*n*-type a-Si:H/Ag/Al. The ZnO:Al and the tin-doped indium oxide (In₂O₃:Sn, ITO) were sputtered by radio-frequency magnetron sputtering using a target of ZnO:Al (1%) and In₂O₃:Sn₂O₃ (10%), respectively. For the textured cell, the ZnO was textured by dipping the sample in a solution of diluted hydrochloric acid (0.5%) for 10 s. Plasma enhanced chemical vapor deposition (PECVD) is used to deposit the doped layers at a radio frequency of 13.65 MHz. Silane (SiH₄) and hydrogen (H₂) are used as source gases. The 25 nm thick *p*-layer and 27 nm thick *n*-doped μ c-Si:H layers were deposited using hydrogen diluted trimethylborane (TMB, 2%) and hydrogen diluted phosphine (2%) as dopant gases, respectively.

Hot-wire chemical vapor deposition (HWCVD) using tantalum wires is used to deposit a 1 μ m thick *i*-layer in 75 minutes¹. These two wires have a diameter of 0.3 mm and are spaced by 3.5 cm, on a distance of 4 cm from the substrate. After the ITO deposition, a short descum process is done to make the surface of the ITO layer hydrophylic using a O₂ -plasma. This improves the adhesion between the liquid silica and the Si surface. The metal back contact was deposited by thermal evaporation Ag and a finishing thin layer of Al to prevent oxidation. The solar cells have an active area of 4 \times 4 mm², which is defined by the mask used for deposition of the metal back contact. Besides the cell area, a manual scribe is done which gives access to the ZnO:Al front contact. Metal is evaporated on top of this scribe, and

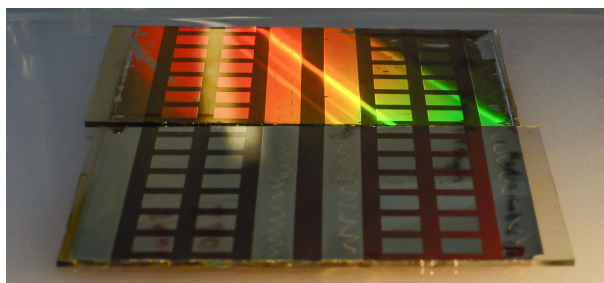


Figure S1: Photo of the backside of the flat (in front) and PSBR (in back) solar cell. The light is scattered by PSBR solar cell resulting in the observed diffraction pattern. The 4 \times 4 mm² squares define the active cell area. The metal stripes at the sides are used to access the ZnO:Al front contacts of the solar cell.

thereby the front ZnO:Al can be contacted via this metal.

Figure S1 shows a sample with flat cells (in front) and with PSBR cells (in back). Due to the periodic pattern of the PSBR the light is scattered. A series of 24 to 30 working solar cells were made for each cell configuration. The reported results are that of the best cell of each configuration.”

2 Internal Quantum Efficiency

Figure S2 shows an indication of the *IQE* of the three different solar cells. The data should be interpreted carefully as the *EQE* and absorptance ($1-R$) are measured using two setups with different optical characteristics. The optical bandwidth from the monochromator of the *EQE* setup is broader than that of the absorptance ($1-R$) setup, resulting in more “smoothing” of the interference fringes of the *EQE* than those of the absorptance (as is indeed visible from the fringe amplitude in Fig. 4 of the paper). Besides this smoothing effect, there are two effects that could contribute to a small wavelength shift of the data of the *EQE* and absorption measurements. (1) The *EQE* and absorptance are measured over a slightly different physical area, which combined with local variations in layer thickness could contribute to a shift of the interference fringes and also some (additional) smoothing. (2) There could be a small wavelength inconsistencies between the absorptance and the *EQE* due to a small wavelength calibration error (in the order of around <10 nm) in the *EQE* setup. Due to a small misalignment of the grating in the monochromator a small wavelength shifts can oc-

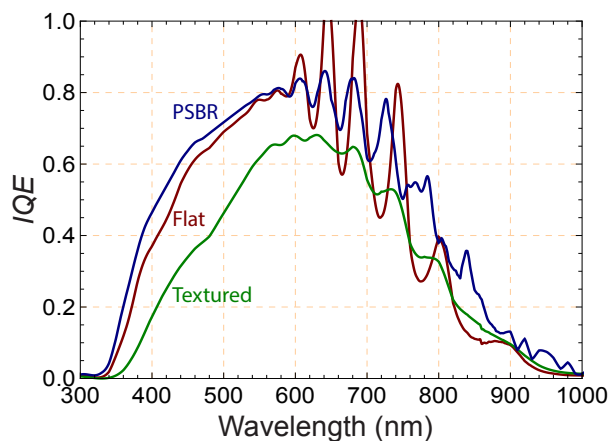


Figure S2: *IQE* of the three different solar cells.

cur.

Due to the sharp interference fringes, these small wavelength shifts result in some errors in the *IQE*. This also explains the unrealistically high *IQE* of more than 1 at two peaks of the curve. However, the global trend of the *IQE* shows that the PSBR and the flat solar cell have a similar *IQE* for wavelengths up to ~ 750 nm.

There is an enhanced *IQE* for wavelengths longer than ~ 750 nm in the PSBR cell as a result of higher effective absorptance due to the light scattering and trapping (the parasitic absorptance and reflection at the front interface stay more or less constant). Moreover, one can observe sharp resonances above 750 nm that are due to additional resonances by the PSBR.

The textured cell has a relatively low *IQE*, especially for wavelengths up to ~ 600 nm. This indicates that the textured cell has poor collection efficiency for charge carriers that are created close the front texture of the solar cell where most of the short wavelength light is absorbed. We expect this to be caused by texture induced defects.

3 Optical Modeling: Particle Swarm Optimization Algorithm

In the simulation we calculate the absorptance in each layer. To calculate the electrical current, we assume that only the charge carriers created in the intrinsic silicon layer are collected at the terminals, and thereby contribute to the J_{sc} . The absorption in the doped layers is considered to be lost due to the high defect density and charge carrier recombination^{2,3}. By integrating the product of the AM1.5G spectrum and the absorptance in the i -layer we calculated the effective photocurrent, which we define as the implied J_{sc} .

A particle swarm optimization (PSO) algorithm⁴ is used to determine the optimal height, diameter, and pitch of the square array of silica nanocylinders. The PSO algorithm scans a defined parameter space, in a similar way as a flock of birds explore an area to find food. When one bird finds food, other birds will likely swarm in the direction of this successful bird to search for food in his neighborhood. At the same time, these exploring birds will plan their flight based on their historical success for finding food at previously visited spots.

To apply this search technique to optimize the current in solar cells, the implied J_{sc} was

set as the figure of merit (FoM)⁵. The PSO algorithm was terminated after 50 generations, with a generation size of 13 individuals. During the last 15 generations the FoM did not change significantly, which indicates that the simulations converged to the optimal geometry. The PSO algorithm saves significant computational power compared to a brute force scan of the parameter space.

References

- (1) Schropp, R. Advances in solar cells made with hot wire chemical vapor deposition (HWCVD): superior films and devices at low equipment cost. *Thin Solid Films* **2002**, *403*, 17–25.
- (2) Luque, A.; Hegedus, S. *Handbook of photovoltaic science and engineering*; John Wiley & Sons, 2011.
- (3) Paetzold, U. W. *Light trapping with plasmonic back contacts in thin-film silicon solar cells*; Forschungszentrum Jülich, 2013.
- (4) Khanna, V.; Das, B.; Bisht, D.; Singh, P. A three diode model for industrial solar cells and estimation of solar cell parameters using PSO algorithm. *Renew Energy* **2015**, *78*, 105–113.
- (5) Robinson, J.; Rahmat-Samii, Y. Particle swarm optimization in electromagnetics. *IEEE T Antenn Propag* **2004**, *52*, 397–407.